REMARKS

Claims 1-11 are pending in the application, and are rejected. Claims 1, 8, 10 and 11 are herein amended. Applicants submit that no new matter has been entered.

Claim Rejections - 35 U.S.C. §102

Claims 8 and 11 are rejected under 35 U.S.C. §102(e) as being anticipated by Nallan et al (US/2004/0002223).

Claims 1 and 10 are herein amended. The amendment finds support in the specification on page 5, lines 11-15. Subsequently, applicants submit that the rejection should be withdrawn because not all of the claimed limitations are taught or suggested by the cited reference.

Applicants note that the intent of the present invention, as clarified by the amendment to claims 8 and 11, is to perform the above steps in order. That is, the region of the film is first exposed to a (N, Ar, or NH_4) plasma, and then it is etched after the plasma treatment. The plasma treatment is done to make the region more easily etched.

The cited reference does not teach this order of steps; rather, the cited reference teaches either (1) the reverse order, or (2) a simultaneous order. That is, the cited reference teaches either (1) performing the steps together in a one-step method, or (2) performing the etching prior to performing the plasma treatment. There is absolutely no teaching or suggestion to employ the steps in the claimed order. Therefore, the rejection over the cited reference should be seen as no longer valid.

Claim Rejections - 35 U.S.C. §103

Claim 9 is rejected under 35 U.S.C. §103(a) as being unpatentable over Nallan et al. (US/2004/0002223), as applied in Paragraph 3 above, and in view of Tsunashima et al. (US/2001/0023120). The Examiner concludes that it would have been obvious to provide Nallan et al. with etching of the insulating layer using sulfuric acid as taught by Tsunashima et al. in order to form a patterned gate stack by using sulfuric acid to etch the amorphous metal oxide layer insulating (gate dielectric film).

Applicants submit that the rejection of claim 8 above has been overcome. Because claim 9 is dependent from claim 8 and necessarily includes at least its limitations, Applicants submit that the rejection of claim 9 has been overcome as well.

Claims 1-3, 7 and 10 are rejected under 35 U.S.C. §103(a) as being unpatentable over Aoyama (US 6,150,221) in view of Callegari et al. (US 6,573,197). The Examiner admits that Aoyama does not specifically disclose the insulating film (i.e., the gate dielectric film) being ZrO_2 or HfO_2. However, the Examiner concludes that it would have been obvious to provide the device of Aoyama where the gate insulating film comprises zirconia or hafnia as taught by Callegari et al. because the high K dielectric layer such as ZrO_2 or HfO_2 are well known in the art.

Claims 4-6 are rejected under 35 U.S.C. § 103(a) as being unpatentable over Aoyama in view of Callegari et al. as applied above, and further in view of Tsunashima et al. The Examiner concludes that it would have been obvious to provide the combination of Aoyama and Callegari et al. with etching of the insulating layer using sulfuric acid as taught by Tsunashima et al. in order to form patterned gate stack by using sulfuric acid to remove (etch) the amorphous metal oxide layer insulating (gate dielectric film).

Applicants respectfully disagree with the above rejections because the cited combination fails to teach or suggest all the limitations of the claimed invention.

Applicants note the Examiner's assertion that Aoyama discloses a method of manufacturing a semiconductor device, the method comprising a step for implanting ions into a region of the insulating film (2) not covered with the mask pattern (3) using the gate pattern as a mask to give damages to the insulating film. The insulating film might be damaged but is not converted into amorphous state. However, according to the description in column 4, lines 29-42 of Aoyama, it is a surface layer of Si-substrate (1) but it is not the insulating film (2) that is converted into amorphous state.

Applicants note that when impurity is implanted by ion implantation, the impurity concentration has a maximum at a certain depth (hereafter referred to as "MAX" depth). The region at the MAX depth and neighborhood thereof are converted into amorphous state. However, a region shallower than the MAX depth region is not converted into amorphous state. U.S. Patent No. 5,468,657 a copy of which being attached hereto, confirms the above. As shown in Fig. 1A, the oxygen ion beam is directed through first surface 22 into the body of substrate 20, which is a wafer of monocrystalline silicon (see column 4, lines 40-46). Implanted ions come to rest in a Gaussian distribution pattern within the substrate, the approximate center of the distribution pattern being at a predetermined depth D (see column 4, lines 53-57). After ion implantation, annealing is carried out (see column 5, lines 36-38). The semiconductor layers 42(20), 44 shown in Figure 1D is still monocrystalline silicon (se column 5, lines 52-53). If the layer 20, which is shallower than the depth D, were converted into amorphous state, the layer 20 could not return to monocrystalline state through annealing. That is, the layer 20 might be damaged, but is not converted into amorphous state.

Applicants note that the Examiner appears to suggest that it would have been obvious that the insulating film (2) shown in Figure 4B of Aoyama is replaced by a ZrO_2 film, which is exemplified as a gate insulating film by Callegari. However, Applicants note that even if the insulating film (2) were replaced by the ZrO_2 film, the ZrO_2 film would not be converted into amorphous state through ion implanting described in Aoyama.

Applicants note that neither Aoyama nor Callegari discloses a step (a3) of claim 1. Claims 2 and 3 depend from claim 1. The step (b3) of claim 7 corresponds to the step (a3) of claim 1.

Applicants note that the preferable condition for transforming the insulating film to an amorphous state is described in line 15-20 on page of the present specification. The preferable acceleration energy is 0.5 keV to 40keV. This range seemingly includes a condition described in lines 35-37 at column 4 of Aoyama. However, in the present invention, the gate insulating film (5) is made of zirconia or hafnia, whereas in Aoyama's embodiment, the gate insulating film (2) appears to be made of silicon oxide. Applicants refer to Figure 2 of IEEE Transactions on Electronics Devices, Vol. 49, No. 10, pp. 1836, a copy of which is attached hereto. When the insulating film to be ion implanted is made of SiO_2, the impurity concentration has a maximum at deeper position than the case where the insulating film is made of HfO_2. In Aoyama's case, even if the acceleration energy is the same, most part of the impurity ions reaches the surface layer of the Si-substrate (1) passing through the insulating film (2). Accordingly, the insulating film (2) is not converted into amorphous state. In contrast, in the present embodiment, more impurity ions come to rest in the insulating film because the insulating film is made of zirconia or hafnia, which it is hard for ions to pass through.

With reference to Tsunashima, comparing claims 4 and 12, the etchant of claim 12 is limited to mixture liquid of sulfuric acid and hydrogen peroxide. Applicants submit that Tsunashima exemplifies sulfuric acid and hydrofluoric acid as the etchant, but does not disclose mixture liquid of sulfuric acid and hydrogen peroxide. The effect obtained by using mixture liquid is described in lines 8-12 on page 6 of the present specification. Therefore, is can be seen that the claimed invention would not be reached even by the proper combination of the cited references.
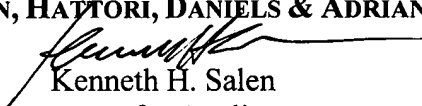
In view of the aforementioned amendments and accompanying remarks, Applicants submit that that the claims, as herein amended, are in condition for allowance. Applicants request such action at an early date.

If the Examiner believes that this application is not now in condition for allowance, the Examiner is requested to contact Applicants' undersigned attorney to arrange for an interview to expedite the disposition of this case.

If this paper is not timely filed, Applicants respectfully petition for an appropriate extension of time. The fees for such an extension or any other fees that may be due with respect to this paper may be charged to Deposit Account No. 50-2866.

Respectfully submitted,

WESTERMAN, HATTORI, DANIELS & ADRIAN, LLP

Kenneth H. Salen
Attorney for Applicants
Registration No. 43,077

KHS/lde
1250 Connecticut Avenue, NW
Suite 700
Washington, D.C. 20036
(202) 822-1100
Enclosures: U.S. Patent No. 5,468,657; IEEE Transactions on Electronics Devices, Vol. 49, No. 10, pp. 1836,

Q:\2003\030862\030862 Amendment 9-29-04.doc

1806

Ion Implantation Impurity Profiles in HfO2

Kunihiro Suzuki and Yusuke Morisaki

Abstract—We implanted B, As, and P ions in a 110-nm-thick layer of HfO2 and extracted the parameters of a Pearson IV function. The projected range of the ion implantation was about half of that in SiO2. Thus, when impurities were ion implanted in an Si substrate through a thin layer of HfO2 or SiO2, a smaller dose was retained in the substrate in the former than in the latter case. This effect was demonstrated with P-ion implantation.

Index Terms—As, B, HfO2, ion implantation, P.

I. INTRODUCTION

HfO2 has a dielectric constant of around 20~30 and is expected to provide one of the main gate-insulator materials for high-speed MOSFETs of the next generation [1]–[3]. HfO2 is expected to realize a SiO2 equivalent gate-insulator thickness of 1 nm. Hence, a typical thickness of HfO2 used in a relevant production is a few nm. Ions are implanted through this layer after the gate-etching process. It is expected from theory that the nuclear interaction between impurities and Hf must be more significant than that between impurities and Si since Hf is heavier than Si [4]. Therefore, the effect of this covering layer on the retained dose or profile should be significant and hence should be investigated. To evaluate this effect, it is important to know the profile in the HfO2. However, accurate evaluation is difficult to perform with a layer of HfO2 that is only a few nm thick.

Here, we deposit a 110-nm-thick layer of HfO2, and implant in it with ions of B, As, and P. We use Pearson IV [5]–[7] (see the Appendix) as a fitting function to express the profiles. We also evaluate the impact of using layers of HfO2 as a covering layer.

II. EXPERIMENT

The substrates were p-type Si(100) wafers having resistivity of 10 Ω-cm. After standard RCA cleaning, 110-nm-thick HfO2 films were deposited by atomic layer chemical vapor deposition (ALCVD) using HfCl4 and H2O at 300 °C. It was confirmed by x-ray diffraction (XRD) that the deposited HfO2 film was an amorphous material, as shown in Fig. 1. Following the deposition, ions of B, As and P were implanted in the layer under a variety of conditions. The depth profiles of B, As, and P implanted in thermally grown SiO2 were also investigated for comparison.

We used a secondary ion mass spectrometer (SIMS) to evaluate the ion-implantation profiles in HfO2 and SiO2. We stopped the SIMS measurement inside the HfO2 layer and measured the depth with a depth profile meter and evaluated the etching rate. We then measured the profile deeper than the HfO2 layer. The depth is calibrated using the etching rate. Therefore, the depth is accurate in the HfO2 layer, but inaccurate in the Si layer. We, therefore, focus on the profiles in the HfO2. We selected the profile where the impurities were well confined in the HfO2 layer and used it as reference data, compared the total counts with dose, obtained the sensitivity factor, and then converted the counts to the concentration. The details of the other conditions for the SIMS measurement are given in Table I.
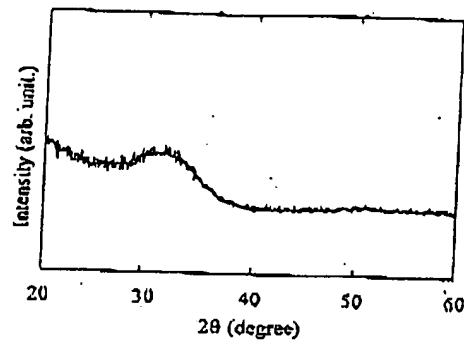
Fig. 1. XDR spectra just after the deposition.

TABLE I
CONDITIONS OF SIMS MEASUREMENT

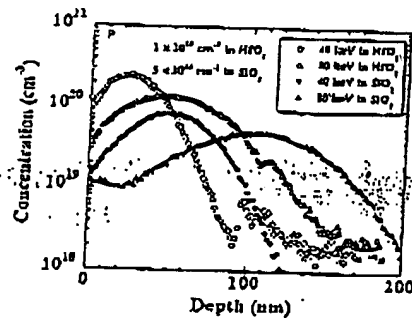| Primary Ion	B	As	P
Primary Ion	O2+	Cs+	Cs+ in HfO2, O2+ in Si
Energy	1 keV for B 3, 5 keV 5 keV for B 10, 20, 40 keV	2 keV for As 5, 10 keV 3 keV for As 20, 40, 80 keV	1 keV
Angle	60°	60°	60°
Vacuum	<1 x 10⁻⁷ Pa	<3 x 10⁻⁷ Pa	<3 x 10⁻⁷ Pa

Fig. 2. SIMS profiles of P concentration in HfO2 and SiO2.

III. RESULTS AND DISCUSSION

Fig. 2 shows SIMS profiles for P implanted in HfO2 and SiO2. The projected range of ions in HfO2 is almost half of that in SiO2. Note that the profile for 80-keV implantation in HfO2 is almost the same as that for 40-keV implantation in SiO2.

Fig. 3 shows the SIMS profiles for B, As, and P implanted in HfO2 at various energies. We fitted the data to the Pearson IV function as an analytical model, focusing on the profile in the HfO2 layer. The results of the analytical model are in good agreement with the experimental data.

Fig. 4 shows the extracted parameters. In all cases, the R_p for HfO2 is about half of the value for SiO2. Therefore, the effective thickness of a layer of HfO2, i.e., the SiO2-equivalent thickness is about twice its physical thickness.

Fig. 5 shows SIMS profiles for P implanted in bare Si and in Si covered by 5-nm-thick layers of HfO2 and SiO2. The impurity profiles were evaluated after removing the covering layers. A much lower dose reaches and remains in the Si substrate with a HfO2 covering layer than with a SiO2 covering layer.
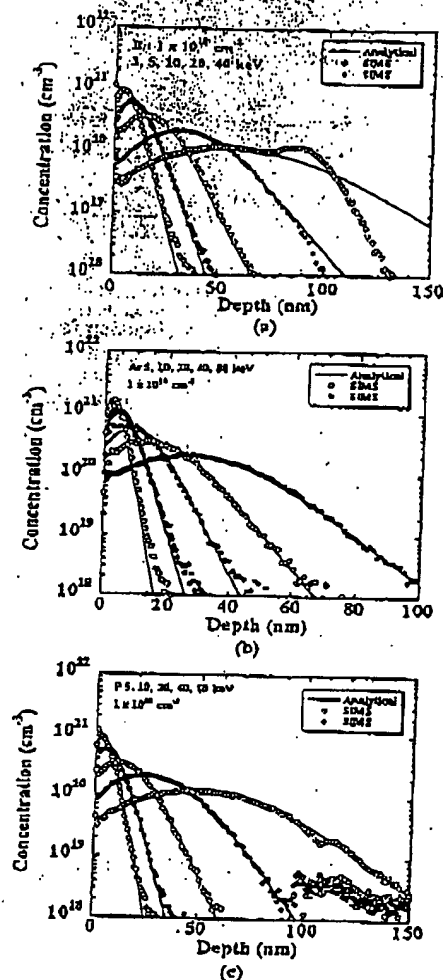
1837

Fig. 3. Comparison of SIMS data and analytical model. (a) B, (b) As, and (c) P.

Fig. 4. Extracted parameters. The R_p values for SiO_2 are also given for comparison. (a) B, (b) As, and (c) P.

The profile in the Si in the multi-layer can be evaluated using a projected range normalized method [8]. In this model, the effective thickness of the cover layer with respect to the Si can be evaluated as
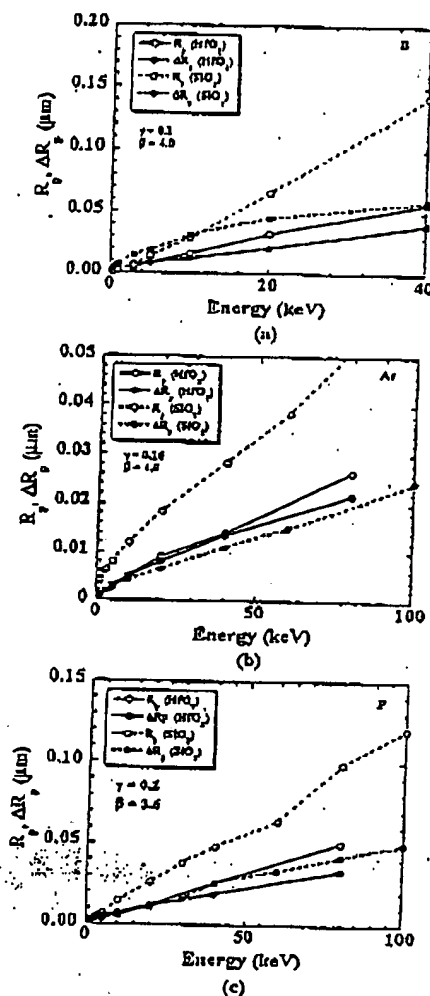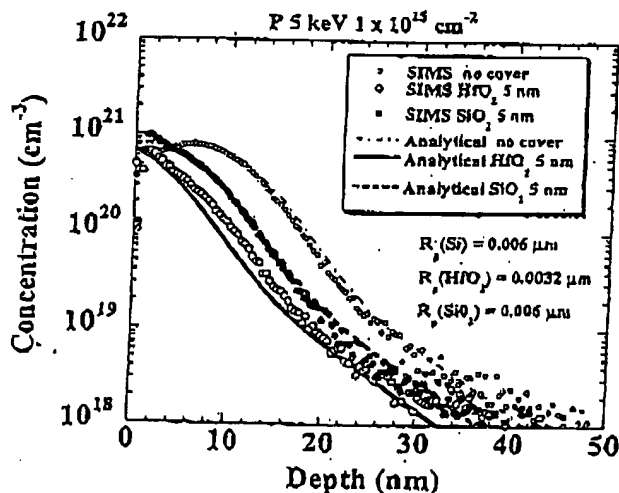
$$d_{eff} = \frac{R_p(Si)}{R_p(HfO_2 \text{ or } SiO_2)} d \qquad (1)$$

where d is the thickness of the covering layer. We consider Si having this thickness to have been deposited on the Si instead of the HfO_2. We generate the ion implantation profile in a single layer of the Si using the parameter in Si. The profile deeper than the effective thickness gives the profile in Si substrates. Fig. 4 shows the analytical model using the treatment of (1).

Fig. 6 shows the cross sectional view of a TEM. We observed the HfO_2 to have a layer thickness of around 5 nm and an interfacial layer of less than 1 nm. If we regard this interface layer as a SiO_2 layer, the effective thickness of (1) should be modified as

$$d_{eff} = \frac{R_p(Si)}{R_p(HfO_2)} d_{HfO_2} + \frac{R_p(Si)}{R_p(SiO_2)} d_{SiO_2}. \qquad (2)$$

The HfO_2 layer thickness d_{HfO_2} was about 5-nm thick and the interfacial layer thickness d_{SiO_2} was about 1-nm thick in our experiment.

Fig. 5. Profiles of P concentration in bare Si and in Si covered by a 5-nm-thick layer of HfO_2 and by a 5-nm-thick layer of SiO_2. SIMS measurements were done after removing covering layers. The results given for the analytical model are also shown.
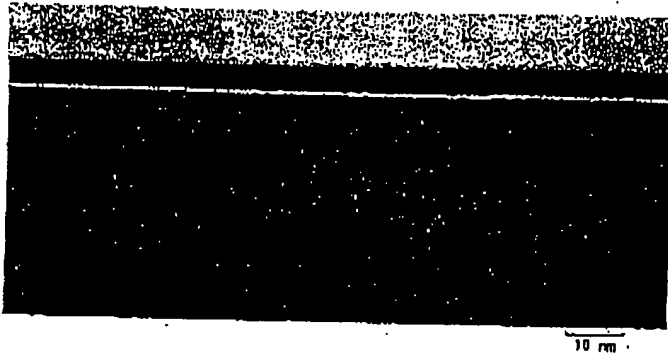
Fig. 6. Cross-sectional view of TEM.

The first term of (2) is 9.3 nm and the latter is 1 nm, hence the interfacial layer does not influence the results significantly. The difference is attributed to the small R_p in HfO$_2$.

When the substrates are subjected to a thermal process, the HfO$_2$ layer becomes crystallized. The ion implantation profile may change correspondingly reflecting the channeling phenomenon. However, we can expect that R_p and ΔR_p are almost the same, while γ and β should be modified depending on the process, which is the case for Si substrates.

IV. CONCLUSION

We implanted ions of B, As, and P in a 100-nm-thick layer of HfO$_2$. We used the Pearson IV function to evaluate the profile, and extracted the corresponding parameters. The projected range of ions in HfO$_2$ is about half of that in SiO$_2$. A much lower dose reaches and is retained in a Si substrate with a covering layer of HfO$_2$ that has a given thickness compared with a covering layer of SiO$_2$ of the same thickness. We demonstrated this with implanted profiles of P ions.

APPENDIX.
THE PEARSON IV FUNCTION

A Pearson function excels in expressing various profile shapes and is given by the solution of the differential equation

$$\frac{dN(s)}{ds} = \frac{(s-a)N(s)}{b_0 + b_1 s + b_2 s^2} \qquad \text{(A-1)}$$

where $s = x - R_p$, and each coefficient is related to the first four moments of the distribution function according to

$$a = -\gamma \Delta R_p (\beta + 3)/A$$
$$b_0 = -\Delta R_p^2 (4\beta - 3\gamma^2)/A$$
$$b_1 = a$$
$$b_2 = -(2\beta - 3\gamma^2 - 6)/A \qquad \text{(A-2)}$$

where $A = 10\beta - 12\gamma^2 - 18$. R_p, ΔR_p, γ and β are related to the moments of the profiles and are given by

$$R_p = \frac{\int_{-\infty}^{\infty} x N(x)\,dx}{\int_{-\infty}^{\infty} N(x)\,dx}, \quad \Delta R_p^2 = \frac{\int_{-\infty}^{\infty} (x - R_p)^2 N(x)\,dx}{\int_{-\infty}^{\infty} N(x)\,dx},$$

$$\gamma = \frac{\int_{-\infty}^{\infty} (x-R_p)^3 N(x)\,dx}{\Delta R_p^3 \int_{-\infty}^{\infty} N(x)\,dx}, \quad \beta = \frac{\int_{-\infty}^{\infty} (x-R_p)^4 N(x)\,dx}{\Delta R_p^4 \int_{-\infty}^{\infty} N(x)\,dx}. \qquad \text{(A-3)}$$

Equation (A-1) gives us various types of function families depending on the relationship between γ and β. Among the Pearson function family, the Pearson IV function is frequently used owing to the fact that it is defined over the entire region and can describe most of the profiles. For Pearson IV condition of $4b_0 b_2 - b_1^2 > 0$, holds, which implies that

$$\beta > \frac{48 + 39\gamma^2 + 6(\gamma^2 + 4)^{1.5}}{32 - \gamma^2}. \qquad \text{(A-4)}$$

Therefore, the function can be expressed by

$$N(s) = K|b_0 + b_1 s + b_2 s^2|^{1/2b_2}$$
$$\cdot \exp\left[-\frac{\frac{b_1}{b_2} + 2a}{\sqrt{4b_0 b_2 - b_1^2}} \tan^{-1}\left(\frac{2b_2 s + b_1}{\sqrt{4b_0 b_2 - b_1^2}} \right) \right] \qquad \text{(A-5)}$$

where K is a factor that has to be determined by equating the integral of (A-5) and the dose.

REFERENCES

[1] K. J. Hubbard and D. G. Schlom, "Thermodynamic stability of binary oxides in contact with silicon," J. Mater. Res., vol. 11, pp. 2757–2776, 1996.

[2] G. D. Wilk, R. M. Wallace, and J. M. Anthony, "High-k gate dielectrics: Current status and materials properties considerations," J. Appl. Phys., vol. 89, pp. 5243–5275, 2001.

[3] C. Hobbs, H. Tseng, K. Reid, B. Taylor, L. Herbert, R. Garcia, R. Hegde, J. Grant, D. Gilmer, A. Franke, V. Dhandapani, M. Azrak, L. Prabhu, R. Rai, S. Bagchi, J. Conner, S. Backer, F. Dumbuya, B. Nguyen, and P. Tobin, "80 nm poly-Si gate CMOS with HfO$_2$ gate dielectric," in IEDM Tech. Dig., 2001, pp. 651–654.

[4] J. Lindhalt, M. Scharff, and H. Schiott, "Range concepts and heavy ion ranges," Mat. Fys. Med. Dan. Vidensk. Selsk, vol. 33, no. 14, 1963.

[5] W. K. Hofker, "Implantation of boron in silicon," Philips Res. Rep. Suppl., vol. 8, pp. 1–121, 1975.

[6] J. P. Biersack, "Basic physical aspects of high energy implantation," Nucl. Instrum. Meth., vol. B35, pp. 205–214, 1988.

[7] D. G. Ashworth, R. Oven, and B. Mundin, "Representation of ion implantation profiles by Pearson frequency distribution curves," J. Phys. D: Appl. Phys., vol. 23, pp. 870–876, 1990.

[8] H. Ryssel, J. Lorentz, and K. Hofmann, "Models for implantation into multi-layer targets," Appl. Phys. A, vol. 41, pp. 201–207, 1986.